Mon. Not. R. Astron. Soc. **000**, 000–000 (2003)

Constraints on a planetary origin for the gap in GM Aurigae's protoplanetary disc

W.K.M. Rice[1], Kenneth Wood[1], P.J. Armitage[2,3], B.A. Whitney[4], J.E.Bjorkman[5]
[1] *School of Physics & Astronomy, University of St Andrews, North Haugh, St Andrews, Kingdom of Fife, KY16 9SS, Scotland*
[2] *JILA, Campus Box 440, University of Colorado, Boulder, CO 80309-0440, USA*
[3] *Department of Astrophysical and Planetary Sciences, Boulder CO 80309-0391, USA*
[4] *Space Science Institute, 3100 Marine Street, Suite A353, Boulder, CO 80303, USA*
[5] *Ritter Observatory, Department of Physics & Astronomy, University of Toledo, Toledo, OH 43606, USA*

12 February 2003

ABSTRACT
The unusual spectral energy distribution (SED) of the classical T Tauri star GM Aurigae provides evidence for the presence of an inner disc hole extending to several au. Using a combination of hydrodynamical simulations and Monte Carlo radiative transport, we investigate whether the observed SED is consistent with the inner hole being created and maintained by an orbiting planet. We show that an $\sim 2M_{\rm Jupiter}$ planet, orbiting at 2.5 au in a disc with mass $0.047M_{\odot}$ and radius 300 au, provides a good match both to the SED and to CO observations which constrain the velocity field in the disc. A range of planet masses is allowed by current data, but could in principle be distinguished with further observations between 3 and $\sim$ 20 microns. Future high precision astrometric instruments should also be able to detect the motion of the central star due to an orbiting Jupiter mass planet. We argue that the small number of T Tauri stars with SEDs resembling that of GM Aur is broadly consistent with the expected statistics of embedded migrating planets.

Key words: radiative transfer — scattering — accretion, accretion disks — ISM: dust, extinction — stars: pre-main-sequence

1 INTRODUCTION

The detection of extrasolar planets and planetary systems (e.g., Mayor & Queloz 1995) has invigorated studies of planetary formation (Lissauer 1993; Boss 1998, 2000), migration (e.g., Lin & Papaloizou 1986; Lin et al. 1996; Trilling et al. 1998; R. Nelson et al. 2000), and interaction with a protoplanetary disc (Lin & Papalizou 1979a, b; Artymowicz & Lubow 1994). Recent theoretical work has investigated mechanisms for halting planetary migration and explaining the statistical distribution of the orbital radii of extrasolar planets (Armitage et al. 2002; Kuchner & Lecar 2002; Trilling, Lunine & Benz 2002). Theoretical models for the interactions of (proto)planets with a protoplanetary disc show that large low density regions (gaps) can be created within the disc (Lin & Papaloizou 1979a, b; Artymowicz & Lubow 1994). The detection of these gaps would provide strong support for planetary formation theories, but current observations do not have the spatial resolution to directly image the au sized gaps that are predicted. Future instrumentation, such as ALMA, may allow direct detection of gaps (Wolf, Henning & Kley 2002), but for now we are restricted to spectral techniques for inferring the presence of disc gaps.

Spectral energy distributions (SEDs) from protoplanetary discs arise from the thermal reprocessing of starlight and dissipation of viscous accretion luminosity (Lynden-Bell & Pringle 1974; Adams, Lada & Shu 1987; Kenyon & Hartmann 1987). The resulting SEDs display characteristic infrared excesses that are sensitive to the size, shape, and mass of the disc. Disc gaps may manifest themselves in SEDs by removing material that would normally have contributed to the SED at a given wavelength: gaps close to the star result in smaller than usual near-IR excesses, while gaps at large disc radii will cause distortions to the SED at longer wavelengths (Beckwith 1999). The classical T Tauri stars GM Aur and TW Hya have SEDs that indicate the inner regions of their discs have been cleared of material out to around 4 au from the central stars (Koerner, Sargent, & Beckwith 1993; Chiang & Goldreich 1999; Schneider et al. 2002; Calvet et al. 2002).

There are a number of possible mechanisms for clearling such gaps. Photoevaporation by ultraviolet radiation, either from the central star or from surrounding radiation, can produce a disc wind at radii where the sound speed exceeds the escape velocity (Clarke et al. 2001). The inner regions of the disc will then be cleared on a viscous timescale

once the wind mass loss rate is comparable to the accretion rate. This, however, generally requires an accretion rate two orders of magnitude lower than the $10^{-8} M_{\odot} \mathrm{yr}^{-1}$ accretion rate expected for GM Aur (Gullbring et al. 1998). Clarke et al. (2001) also assumed a constant ionizing flux. Matsuyama et al. (2002) show that the clearing of the inner disc is even less likely if the decrease in ionizing flux with decreasing accretion rate is included in the calculation. A. Nelson et al. (2000) also suggest that viscous dissipation and the dissipation of gravitational instabilities may increase the midplane temperature of the inner regions of the disc to above the grain destruction temperature. This would then manifest itself as a reduction in the flux of radiation with wavelengths between a few and ten microns. Their simulation, however, assumed a disc luminosity ($0.5 L_{\odot}$) an order of magnitude greater than that calculated by Gullbring et al. (1998) for GM Aur ($0.071 L_{\odot}$).

It has been suggested (Calvet et al. 2002) that the inner regions of TW Hydra's disc could be cleared by tidal interactions with an embedded planet (Lin & Papalizou 1979a, b). In this paper we consider if the gap in GM Aur's disc could be formed in the same way. We use a dynamical model of an approximately Jupiter mass planet in a protoplanetary accretion disc, with parameters appropriate for GM Aur (e.g., Koerner, Sargent & Beckwith 1993; Simon, Dutrey & Guilloteau 2000; Schneider et al. 2002), to investigate if the resulting disc structure can reproduce the observed SED. We also consider other planet masses to test if the SED can be used to constrain the planet mass. Estimates for GM Aur's age vary from ~ 1.5 Myr (Beckwith et al. 1990; Siess, Forestini & Bertout 1999) to ~ 10 Myr (Simon & Prato 1995; Hartmann 2002). There has therefore been sufficient time for an embedded planet to have formed via core accretion (Lissauer 1993) or via gravitational collapse (Boss 1998, 2000). The observation of a much younger system (e.g., < 1 Myr) with an SED signature indicating the presence of a disc gap would, if the gap could be shown to be due to the presence of an embedded planet, suggest that either core accretion occurs on a much shorter timescale than expected or that planet formation can occur via an alternative mechanism such as gravitational collapse. In section 2 we describe and present the results of our dynamical simulations, in § 3 we compare model SEDs with the observed SED of GM Aur, and we summarize our results in § 4.

2 DYNAMICAL SIMULATIONS

2.1 Dynamical Model and Initial conditions

The simulations presented here were performed using smoothed particle hydrodynamics (SPH), a Lagrangian hydrodynamics code (e.g., Benz 1990; Monaghan 1992). We initially assume a planet with mass $M_p = 1.7 M_J$ orbits a star, with mass $M_* = 0.85 M_{\odot}$, at a radius of $r_p = 2.5$ au. Both the central star and planet are modelled as point masses onto which gas particles can accrete if they approach to within the sink radius (Bate et al. 1995). The planet orbits within a circumstellar disc of mass $M_{\rm disc} = 0.047 M_{\odot}$, modelled using 300000 SPH gas particles distributed such as to give a surface density profile of $\Sigma \propto r^{-1}$ (D'Alessio et al. 1998). The disc extends from $r_{\rm in} = 0.25$ au to $r_{\rm out} = 300$ au. The disc temperature varies as $T \propto r^{-1/2}$, as expected for discs heated by starlight (D'Alessio et al. 1998), and we assume hydrostatic equilibrium in the vertical direction, giving a central density profile of $\rho \propto r^{-2.25}$. For the SPH simulation, the disc is assumed to be locally isothermal and the above temperature profile is maintained throughout the simulation. The parameters chosen are appropriate for GM Aur based on calculations of the stellar mass (Simon, Dutrey & Guilloteau 2000) and the disc mass and size (Schneider et al. 2002).

The vertical scale height, H, of the disc is given by $H^2 = c_s^2 r^3 / G M_*$ where c_s is the local sound speed, r is the radius, G is the gravitational constant, and M_* is the stellar mass. The temperature is normalised such as to give a scale height of 10.5 au at 100 au. The scale height at 2.5 au is then 0.1 au, giving an H/r value of 0.04. This choice of scale height was based on an SED model using an analytic disc geometry and is similar to that obtained by Schneider et al.(2002). In using the above form for the scale height, we assume that the dust has the same scale height as the gas. Although this may not necessarily be the case, the need to use a dust scale height that has the same form as a standard equilibrium disc (e.g., Pringle 1981) would seem to make this a reasonable assumption.

Using 300000 SPH particles the vertical profile of the disk can be modelled accurately within ~ 3 scale heights of the disc midplane. For higher altitudes, the density is calculated analytically using (e.g., Pringle 1981)

$$\rho(z, r) = \rho_c(r) \exp(-\mathrm{z}^2 / 2\mathrm{H}^2) \quad (1)$$

where z is the height above the disc midplane, and $\rho_c(r)$ is the central density a distance r from the central star, determined using the dynamical model. Very little mass is contained in these regions of the disc and is hence unimportant for the dynamical calculation. It is, however, extremely important for calculating the radiative transfer through the disc (see D'Alessio et al. 1998).

Self-gravity is included in the calculation and both the point masses and the gas use a tree to calculate gravitational forces (Benz et al. 1990). The inclusion of self-gravity means that the central star and planet are both free to move under the gravitational influence of the disc. A great saving in computational time is obtained by using individual, particle time-steps (Bate et al. 1995; Navarro & White 1993) which are limited by the Courant condition and a force condition (Benz et al. 1990).

2.2 Planet-disc interactions

A planet orbiting within a circumstellar disc will tidally interact with the disc. Disc material exterior to the planet will gain angular momentum from the planet and will move to larger radii, while material interior to the planet will lose angular momentum and move to smaller radii (Lin & Papaloizou 1979a, b; Artymowicz & Lubow 1994). Viscous processes within the disc will tend to act against the tidal forces and the formation of a gap will depend on the tidal forces overcoming these viscous processes (Lin & Papaloizou 1979a). This depends on the relative magnitudes of the mass ratio of the planet and the star, q, and the Reynolds number within the disc, $\mathcal{R}$. If $q > \mathcal{R}^{-1}$ a gap will form, while if

$q^2 > \mathcal{R}^{-1}$ the disc will be truncated at the outer Lindblad resonance. The Reynolds number is given by $\Omega r^2/\nu$ where Ω is the angular frequency, r is the radius, and ν is the turbulent viscosity in the disc generally described as an alpha viscosity (Shakura & Sunyaev 1973).

For the initial simulation ($M_p = 1.7M_J$, $M_{\rm disc} = 0.047M_\odot$) considered here $q = 0.002$, and the Reynolds number, determined from the artificial viscosity included in the code (Murray 1996), is ~ 20000. Therefore $q > \mathcal{R}^{-1}$ but $q^2 < \mathcal{R}^{-1}$. A gap should form with the gap edge at the outer Lindblad resonance located, for a planet orbiting at 2.5 au, at a radius $r = 4$ au. However, for the mass ratio and Reynolds number in this initial simulation, the disc should not be strongly truncated at the outer Lindblad resonance. The Lindblad resonance can be determined from $\Omega(r) = \omega m/(1+m)$ where ω is the angluar frequency of the orbiting planet and, for the outer Lindblad resonance, $m = 1$ (Binney & Tremaine 1987; Lin & Paploizou 1979a). The angular frequency at the outer Lindblad resonance is therefore $\Omega(r) = \omega/2$. The assumption of a planet orbiting at 2.5 au was based on SED calculations using an analytic disc geometry and the results of Schneider et al.(2002) which suggest that the best fit to the SED occurs for gap extending to a radius of 4 au (i.e., the radius of the outer Lindblad resonance for a planet orbiting at 2.5 au).

Figure 1 shows the azimuthally averaged midplane density at the beginning (dashed line) and end (solid line) of the simulation. After 1820 years the planet orbiting at 2.5 au has produced a gap in the disc out to $r \approx 4$ au. The gap edge is relatively soft, consistent with the relative magnitudes of the mass ratio (q) and Reynolds number ($\mathcal{R}$). The softness of the gap edge is likely to have an impact on the radiation transfer through the disc. As will be considered in a later section, to produce a gap with a significantly harder edge would require a more massive companion or a significantly less viscous disc. The mass within 5 au has reduced from $4 \times 10^{-4} M_\odot$ at $t = 0$ to $4 \times 10^{-5} M_\odot$ at $t = 1820$ years. The reduction in the number of SPH particles respresenting the gas within 5 au requires the use of equation 1 to determine the vertical density at distances greater than 1 scale height above the disc midplane.

If the planet clears sufficient material from within its orbit, torques from material outside its orbit should cause it to eventually lose angular momentum and spiral inwards. However, the planet in this simulation is approximately four times as massive as the disc material contained within its orbit and hence we expect it to suffer minimal orbital migration (Syer & Clarke 1995; R. Nelson et al. 2000).

Accretion onto the central star and the orbiting planet continues throughout the simulation despite the formation of the gap, consistent with simulations performed by Artymowicz & Lubow (1996). The central star has increased from it's initial mass of $0.85M_\odot$ to a mass of $0.85019M_\odot$ after 1820 years, while the orbiting planet has increased from $1.7 \times 10^{-3} M_\odot$ to $1.88 \times 10^{-3} M_\odot$ in the same time period. The accretion rate at the end of the simulation (averaged over the last 100 years) was $\sim 5 \times 10^{-8} M_\odot {\rm yr}^{-1}$ and $1 \times 10^{-8} M_\odot {\rm yr}^{-1}$ for the central star and orbiting planet respectively. An accurate calculation of the accretion rate in our simulation is limited by the mass resolution, since each SPH particle has a mass of $1.6 \times 10^{-7} M_\odot$, and by our simplistic accretion process. We do not include the rotating magnetosphere of the T Tauri star which is likely to truncate the disc at the corotation radius and force the accretion flow to follow the stellar magnetic field lines (Ghosh & Lamb 1978). The accretion rate from the model is however similar to that expected for GM Aur (Gullbring et al. 1998). That mass is flowing through the gap and accreting onto the central star and planet is also consistent with other simulations (Artymowicz & Lubow 1996; Lubow et al. 1999).

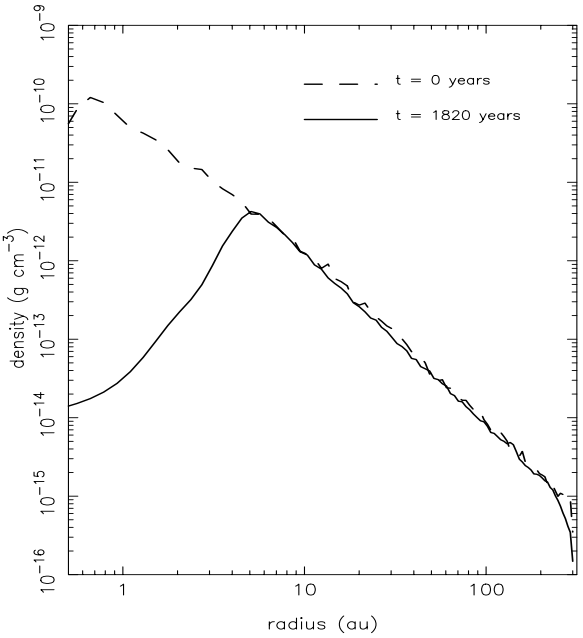

Figure 1. Azimuthally averaged midplane disc density at the beginning (dashed line) of our simulations and after the $1.7M_J$ planet has completed 450 orbits at 2.5 au (solid line).

The disc velocities also remain very close to Keplerian despite the presence of an orbiting planet that perturbs the potential. This is consistent with CO observations (Koerner, Sargent & Beckwith 1993; Dutrey et al. 1998) which suggest that GM Aur is surrounded by a Keplerian circumstellar disc inclined at $\sim 50°$.

3 RADIATION TRANSFER MODELS

We calculate the SED for our simulations using the Monte Carlo radiative equilibrium technique of Bjorkman & Wood (2001). The output of our radiative transfer simulation is the disc temperature structure and the emergent SED. The disc heating is assumed to be from starlight and the Monte Carlo "photons" are tracked within a two dimensional grid in r and θ. Our radiation transfer code calculates disc temperature and does not assume a vertically isothermal structure as in the SPH simulation. The input stellar spectrum is a 4000K, $\log g = 3.5$ Kurucz model atmosphere (Kurucz 1994) and the stellar radius (R_*) is taken to be 1.75 $R_\odot$. The circumstellar dust opacity is taken to be that described in Wood et al. (2002a) which fits the HH 30 IRS SED and was also

used to fit the GM Aur SED (Schneider et al. 2002). The dust model has a shallower wavelength dependent opacity than "standard" ISM dust (e.g., Mathis, Rumpl, & Nordsieck 1977) and a larger grain size as inferred for many other classical T Tauri stars (e.g., Beckwith et al. 1990; Beckwith & Sargent 1991).

We find that the dearth of near-IR excess in GM Aur's SED cannot be explained by a dust composition different to that used here. Using an ISM mixture and a disc without a substantial gap still results in a near-IR excess not observed in GM Aur. Our results are also in agreement with the Calvet et al. (2002) modelling of TW Hya. In their model they do use different dust types in the inner and outer disc, but still require a very low density inner disc to reproduce the near-IR emission observed in TW Hya. Further, ISM grains yield too steep a slope to the sub-mm SED (see also Beckwith & Sargent 1991). We therefore conclude that the dearth of near-IR excess emission from GM Aur can only be explained by an evacuated (low density) inner region.

Circumstellar discs absorb and reprocess stellar photons in a layer which, depending on the disc optical depth, can lie four to five scaleheights above the disc midplane (D'Alessio et al. 1999). Our SPH simulations cannot resolve this low density material, so to provide a density grid for our radiation transfer simulations we have extrapolated the density, using Equation (1), to large heights above the disk midplane. The density calculated from the SPH simulations was azimuthally averaged and then interpolated onto a two dimensional grid in r and θ. The grid has 100 cells for $0.25\text{au} \leq r \leq 300\text{au}$ spaced proportional to r^3 and 400 cells linearly spaced for $0 \leq \theta \leq \pi$. This gridding allows us to adequately resolve the SPH density for our SED calculations.

3.1 GM Aur SED

Figure 2 shows the GM Aur SED data. The dotted line shows the input model atmosphere, and the open squares are data points obtained using various instruments (e.g., Cohen & Kuhi 1979; Kenyon & Hartmann 1995; Weaver & Jones 1992; Beckwith & Sargent 1991). The solid line shows the SED calculated using the azimuthally averaged SPH density as input to the Monte Carlo radiation transfer calculation. The SPH simulation was run for 450 orbits of the 1.7 Jupiter mass planet at 2.5 au (1820 years), giving sufficient time for the density profile to reach a steady state. The disc structure is also approximately azimuthally symmetric since the viscous timescale is significantly greater than the planet's orbital period. The inclination of the disc was taken to be 50°, consistent with the value of $54° \pm 5°$ determined by Dutrey et al. (1998), and with the recent scattered light models of Schneider et al. (2002). The model SED provides a good fit to the observations, particularly the lack of near-IR excess and the level and slope of the long wavelength continuum. The dashed line in Figure 2 is the SED for an equivalent disc in which a gap is not present and in which the inner edge of the disc is taken to be at 7 stellar radii. Comparison between the solid line and dashed line clearly shows that the effect of the disc clearing is to reduce the excess emission at short wavelengths ($2 - 10$ microns) and slightly increase the excess at longer wavelengths ($10 - 30$ microns).

This is consequence of the stellar flux being reprocessed

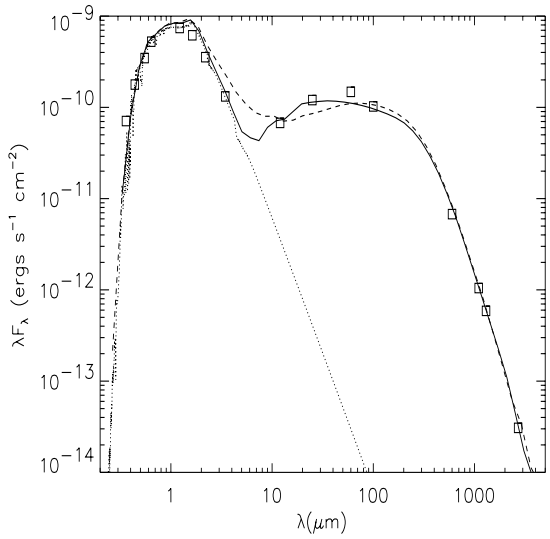

Figure 2. GM Aur's spectral energy distribution (squares), our model viewed at $i = 50°$ (solid line) and input stellar spectrum (dotted line). The dashed line shows the SED calculated in the absence of a gap with the disc extending in to 7 stellar radii. The presence of a gap (solid line) clearly reduces the near infra-red flux and enhances the flux at slightly longer wavelengths.

at the disc edge. In the simulation with $R_{\min} = 7R_*$ (dashed line in Figure 2) stellar photons are reprocessed in high temperature (> 1000 K) regions of the disc giving a near-IR excess. When a gap is present the photons are reprocessed further out in the disc where the temperature is lower, decreasing the near infrared flux and increasing the flux at longer wavelengths. A fit to the data is only possible if the gap extends all the way to the inner disc boundary. If the planet has only had sufficient time to clear a ring of material, leaving the inner disc almost unchanged, this inner material should remain hot, resulting in 2 and 3 micron fluxes similar to that for the dashed line in Figure 2, and higher than that observed for GM Aur (open squares).

3.2 Companion (planet) mass and viscosity

Although we are able to reproduce the observed SED with a 1.7 Jupiter mass planet orbiting at 2.5 au, the exact form of the density profile depends on the relationship between the mass ratio, q, and the disc Reynolds number, $\mathcal{R}$. A weakness of SPH is the difficulty in determining exactly the viscosity and hence Reynolds number. In light of this, we have performed a number of additional simulations considering substellar companions (planets) of various masses, each of which was run for at least 250 orbits of the companion around the central star (> 1000 years). In these simulations the disc was modelled between 0.25 and 100 au using 150000 SPH particles with a surface density profile such that the total disc mass would be $0.047M_\odot$ were the disc extended to 300 au. Using 150000 SPH particles to simulate the inner 100 au of the disc should give approximately the same resolution as the 300000 particles used to simulate the disc out to 300 au. The Reynolds number in the simulations using 150000 SPH particles should therefore be very similar to the Reynolds

number in a 300000 particle simulation (Murray 1996). The companion masses considered for these additional simulations were 0.085, 21, and $43M_J$. In simulating companions with relatively large masses (21 and $43M_J$) we are not necessarily suggesting that one would expect to observe substellar companions with such masses, but simply illustrating how the SED can vary with mass. Strictly speaking, such massive objects would generally be regarded as brown dwarfs, and we therefore refer to the 21 and $43M_J$ companions as substellar objects rather than planets.

The process of star formation is known to preferentially produce binary stellar systems rather than single stars (Duquennoy & Mayor 1991). On the main sequence, however, the mass ratio of close binaries is rarely so extreme as to pair a Solar mass star with a brown dwarf (Marcy & Butler 2000; Halbwachs et al. 2000). If this trend also exists during the pre-main-sequence phase, one would expect disc-embedded planetary mass objects to be more common than embedded close brown dwarfs. The formation mechanism of close binaries is, however, unclear with some simulations (Bate, Bonnell & Bromm 2002) suggesting substantial evolution of binary orbital parameters while a disc is present. The possibility of observing substellar mass companions at this early stage could therefore be an important test of different binary formation models.

The Reynolds number, $\mathcal{R}$, in the disc is calculated to be ~ 20000. The 0.085 and 1.7 Jupiter mass planets therefore have $q > \mathcal{R}^{-1}$ but $q^2 < \mathcal{R}^{-1}$ while the 21 and 43 Jupiter mass substellar objects have $q > \mathcal{R}^{-1}$ and $q^2 > \mathcal{R}^{-1}$. The two planets (0.085 and $1.7M_J$) should therefore produce gaps that are not strongly truncated at the outer Lindblad resonance while the two substellar objects (21 and $43M_J$) should truncate the disc strongly at the outer Lindblad resonance (Lin & Papaloizou 1979a; Syer & Clarke 1995). For a Reynolds number larger than used here, a planetary mass companion ($< 10M_J$) would satisfy easily the latter condition ($q > \mathcal{R}^{-1}$ and $q^2 > \mathcal{R}^{-1}$). The results we obtain for the companions referred to as substellar objects would therefore also be applicable to planetary mass objects in a disc with a Reynolds number larger than in the simulation presented here.

Figure 3 shows the azimuthally averaged midplane densities for the three additional masses together with the azimuthally averaged midplane density profile for the $1.7M_J$ planet, between radii of 0.25 and 25 au. As expected the 0.085 and 1.7 Jupiter mass planets produce gaps with soft edges while the 21 and 43 Jupiter mass objects truncate the disc strongly at the outer Lindblad resonance. The position of the gap edge varies slightly for the different masses, but in all cases is close to the outer Lindblad resonance at ~ 4 au.

Figure 4 shows the SEDs calculated using the azimuthally averaged density profiles for the four masses as input to the radiation transfer calculation. Since the simulations considering masses of 0.085, 21, and $43M_J$ were only performed out to 100 au, the density profiles were extrapolated to 300 au. The solid and dotted lines are for the $1.7M_J$ and $0.085M_J$ planets, while the dashed and dash-dot lines are for the $43M_J$ and $21M_J$ substellar objects. The SEDs for the 1.7 and $0.085M_J$ planets are very similar, as are the SEDs for the two substellar objects (21 and $43M_J$), which are, in fact, very difficult to separate. Figure

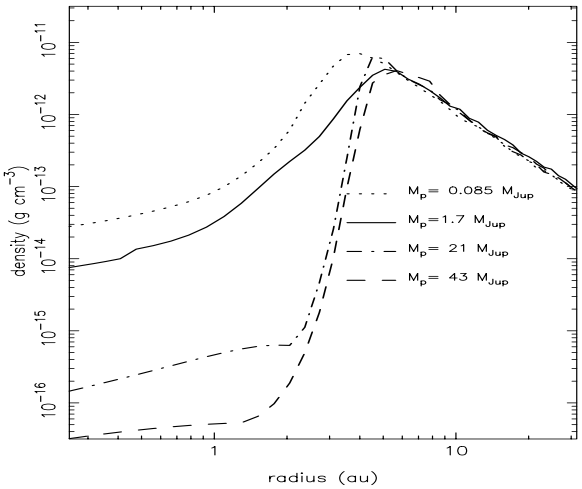

Figure 3. Azimuthally averaged midplane density profiles for substellar objects (planets) with masses of 0.085 (dotted line), 1.7 (solid line), 21 (dash-dot line), and 50 M_J (dashed line). The two higher mass objects truncate the disc more strongly at the outer Lindblad resonance than the two lower mass planets.

5 shows a detailed view of the computed SEDs between 5 and 200 microns with the line styles the same as in Figure 4. Figure 5 also shows ± 25 % error bars on the data points (open squares). This choice of error was based on worst case 1 σ error estimates (Cohen & Kuhi 1979; Weaver & Jones 1992; Kenyon & Hartmann 1995). Apart from the SED flux at 12 microns due to the $0.085M_J$ planet (dotted line) being slightly higher than that observed, the SEDs computed from the density profiles fit the 2, 3, and 12 micron data points well. The flux between 3 and 12 microns varies quite considerably for the different masses, suggesting that more observations in this wavelength range could allow for the determination of the companion mass or, since the Reynolds number in the disc is unlikely to be accurately known, the relationship betwen the mass ratio and the Reynolds number. The SEDs due to the 21 and $43M_J$ substellar objects also have a flux at 25 microns that is considerably higher than that observed. Although not definitive, this may suggest that if the GM Aur SED is due to an embedded companion (planet) orbiting at ~ 2.5 au, the mass must be such as to produce a gap that is not strongly truncated at the outer Lindblad resonance, i.e. $q > \mathcal{R}^{-1}$ but $q^2 < \mathcal{R}^{-1}$. This also appears to be the case for TW Hydra as Calvet et al. (2002) require low density material within 4 au to fit the $2 - 10$ micron SED flux.

At the distance of GM Aur (140 pc), a few Jupiter mass planet orbiting at 2.5 au will produce a 'wobble' in the central star with an angular displacement of ~ 0.1 milliarcsec, and a period of 4 years. Future high precision astrometric instruments should be sufficiently sensitive to make such an observation. Observations of this kind have been suggested for detecting both the presence of embedded planets (Boss 1998) and for detecting instabilities in self-gravitating protoplanetary discs (Rice et al. 2002).

Although it is difficult in SPH both to determine and

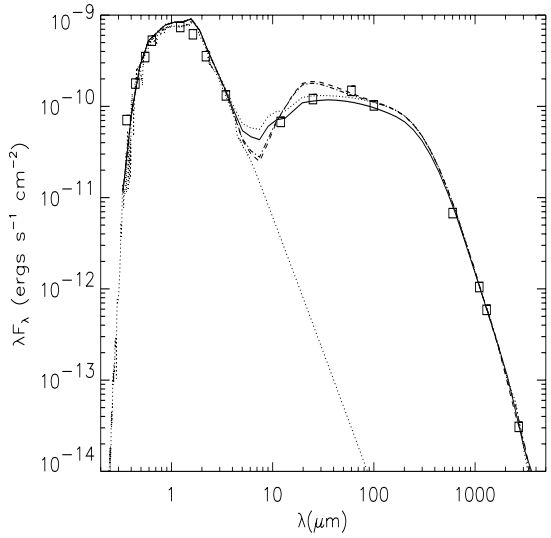

Figure 4. GM Aur's SED computed using the azimuthally averaged density profiles due to planets with masses of 0.085 (dotted line), 1.7 (solid line) and substellar companions with masses of 21 (dash-dot line) and $43M_J$ (dashed line), as input to the Monte Carlo radiation transfer.

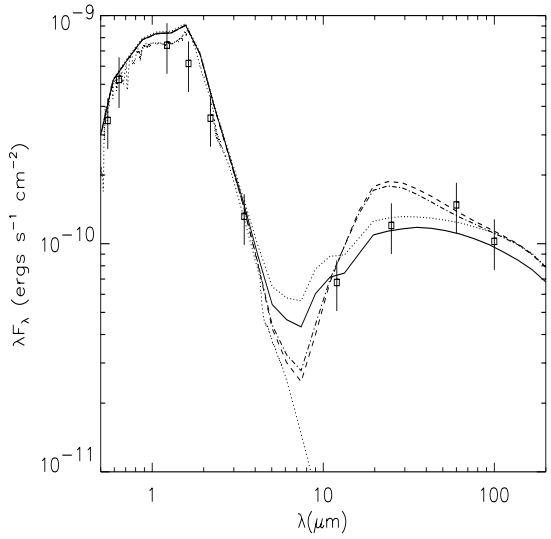

Figure 5. Detailed view of the computed SEDs between 5 and 200 microns. The line styles correspond to embedded planet masses of 0.085 (dotted line), 1.7 (solid line), 21 (dash-dot line), and $43M_J$ (dashed line). Error bars have been added to the data points with the error ($\pm$25 %) based on worst case error estimates.

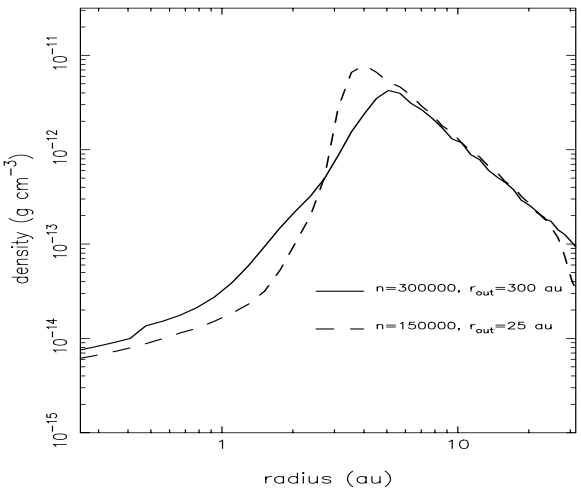

Figure 6. Azimuthally averaged midplane density profiles for a disc modelled, between 0.25 and 300 au using 300000 SPH particles (solid line), and one modelled between 0.25 and 25 au using 150000 SPH particles. The higher resolution simulation has a larger Reynolds number and hence, even though both simulations have the same planet mass ($1.7M_J$), the gap is slightly harder than the lower resolution simulation.

set the viscosity, by performing a number of simulations with various companion masses we are able to determine how the density profile, and resulting SED, varies for various values of the mass ratio to Reynolds numbers ratio. To further test the relationship between planet mass and viscosity we have also performed a high resolution SPH simulation using 150000 SPH particles to simulate the inner 25 au of the accretion disc. This increases the Reynolds number by a factor of 2 and allows the inner few au of the disc to be represented by more SPH particles once the gap has formed. Figure 6 shows the midplane disc density for the simulation using 300000 particles to represent the entire disc (solid line) and the simulation using 150000 particles to respresent the inner 25 au (dashed line). In both cases a planet mass of $1.7M_J$ was used. Although the density profiles differ, this is entirely consistent with the increased Reynolds number of the high resolution simulation. Extrapolating the high resolution simulation to 300 au and using the resulting density profile as input to the radiation transfer produces an SED that, like the previous 0.085 and $1.7M_J$ simulations, fits the data remarkably well.

4 SUMMARY

We have presented an SPH simulation of a planet opening up a gap in GM Aur's protoplanetary disk. For a $1.7M_J$ planet orbiting at 2.5 au, the disc density within 4 au is decreased by three orders of magnitude. The almost Keplerian velocity structure matches that derived from CO observations. Further, our radiation transfer simulations of a passively heated disk show that the disc structure from the SPH simulation reproduces the observed SED of GM Aur.

Additional simulations of companions (planets) with masses of 0.085, 21, and $43M_J$ were also performed. The structure of the resulting gaps depend on the relationship between the mass ratio and the Reynolds number in the disc. For the Reynolds number in our simulations, the two planets (0.085 and $1.7M_J$) produce gaps with relatively soft edges, while the two substellar objects (21 and $43M_J$) truncate the disc strongly at the outer Lindblad resonance (~ 4 au). As with the $1.7M_J$ planet, the SED computed using the density profile due to the $0.085M_J$ planet fits the data points extremely well. The SEDs computed using the density profiles due to the two substellar objects (21 and $43M_J$) fit most data points well but have quite a significant excess at 25 microns. Although not definitive, this may suggest that the mass must be such as to produce a gap that is not strongly truncated at the outer Lindblad resonance. Further observations between 3 and 20 microns, where there is a considerable difference in the computed SEDs, but currently no data points, will be needed to determine if this is indeed the case. Future SIRTF observations will provide the required measurements to test our predictions.

Since the density profile depends on the relationship between the mass ratio and the Reynolds number, additional information would be required to determine the actual planet mass. A few Jupiter mass planet orbiting at 2.5 au will produce a 'wobble' in the central star, at the distance of GM Aur (140 pc), with an angular displacement of ~ 0.1 milliarcsec, and a period of 4 years. Future high precision astrometric instruments should be sufficiently sensitive to make such observations. Not only would this establish if a planet is indeed orbiting at ~ 2.5 au but should also allow for the determination of the planet mass from which the Reynolds number, and hence the turbulent viscosity, could be estimated.

The transfer of angular momentum between the embedded planet and the disc material is ultimately expected to cause the planet to migrate inwards (Lin & Paploizou 1986). Simulations (R. Nelson et al 2000) suggest that the migration timescale is of order 10^5 yrs for a Jupiter mass planet starting at 5 au. Since as many as 15 percent of Solar type stars are expected to have planets within 5 au, that there are only currently two T Tauri stars with SED signatures of close-in massive planets is somewhat surprising. This could reflect the relatively sparse observations in the relevant wavelength range ($3 - 12$ microns). Alternatively, fully evacuated inner holes may form in only a fraction of classical T Tauri stars with planets. An annular gap with a sizeable inner disc would lead to less obvious signatures in the SED.

acknowledgements

We acknowledge financial support from a PPARC standard grant (WKMR) and Advanced Fellowship (KW). BW would like to acknowledge support from NASA's Long Term Space Astrophysics (LTSA) Research Program, NAG 5-8412.

REFERENCES

Adams F.C., Lada C.J., Shu F.H., 1987, ApJ, 312, 788.
Armitage P.J., Livio M., Lubow S.H., Pringle J.E., 2002, MNRAS, 334, 248
Artymowicz P., Lubow S.H., 1994, ApJ, 421, 651.
Artymowicz P., Lubow S.H., 1996, ApJ, 467, L77.
Bate M.R., Bonnell I.A., Bromm V., 2002, MNRAS, 336, 705.
Bate M.R., Bonnell I.A., Price N.M., 1995, MNRAS, 277, 362.
Beckwith S.V.W., 1999, in "The Origin of Stars and Planetary Systems," ed. C.J. Lada & N.D. Kylafis, Kluwer, 579
Beckwith S.V.W., Sargent A.I., 1991, ApJ, 381, 205
Beckwith S.V.W., Sargent A.I., Chini R.S., Gusten R., 1990, AJ, 99, 924
Benz W., 1990, in Buchler J.R., ed, The Numerical Modeling of Nonlinear Stellar Pulsations, Kluwer, Dordrecht, p. 269.
Binney J., Tremaine S., 1987, Galactic Dynamics, Princeton University Press, Princeton.
Bjorkman J.E., Wood K., 2001, ApJ, 554, 615
Boss A.P., 1998, Nature, 393, 141.
Boss A.P., 2000, ApJ, 553, 174.
Calvet N., D'Alessio P., Hartmann L., Wilner D., Walsh A., Sitko, M., 2002, ApJ, 568, 1008
Cardelli J.A., Clayton G.C., Mathis J.S., 1989, ApJ, 345, 245
Chiang E.I., Goldreich P., 1999, ApJ, 519, 279
Clarke C.J., Gendrin A., Sotomayor M., 2001, MNRAS, 328, 485.
Cohen M., Kuhi L.V., 1979, ApJS, 41, 743
D'Alessio P., Canto J., Calvet N., Lizano S., 1998, ApJ, 500, 411.
D'Alessio P., Calvet N., Hartmann L., Lizano S., Canto, J., 1999, ApJ, 527, 893
D'Angelo G., Henning T., Kley W., 2002, A&A, 385, 647
Duquennoy A., Mayor M., 1991, A&A, 248, 485.
Dutrey A., Guilloteau S., Prato L., Simon M., Duvert G., Schuster K., Menard F., 1998, A&A, 338, L63.
Ghosh P., Lamb F.K., 1978, ApJ, 233, L83.
Goldreich P., Tremaine S., 1980, ApJ, 241, 425
Gullbring E., Hartmann L., Briceno C., Calvet N., 1998, ApJ, 492, 323.
Halbwachs J.-L., Arenou F., Mayor M., Udry S., Queloz D., 2000, A&A, 355, 581.
Haisch K.E., Lada E.A., Lada C.J., 2001, ApJ, 553, L153
Hartmann L., 2002, ApJ, in press.
Kenyon S.J., Hartmann L., 1987, ApJ, 323, 714
Kenyon S.J., Hartmann L., 1995, ApJS, 101, 117.
Koerner D.W., Sargent A.I., Beckwith S.V.W., 1993 Icarus, 106, 2
Kuchner M.J., Lecar M., 2002, ApJ, 574, L87.
Kurucz R.L., 1994, CD-ROM 19, Solar Model Abundance Model Atmospheres (Cambridge: SAO)
Lin D.N.C., Papaloizou J., 1979a, MNRAS, 186, 799.
Lin D.N.C., Papaloizou J, 1979b, MNRAS, 188, 191.
Lin D.N.C., Papalizou J., 1986, ApJ, 309, 846.
Lin D.N.C., Bodenheimer P., Richardson D.C., 1996, Nature, 380, 606
Lissauer J.J., 1993, ARA&A, 31, 129.
Lubow S.H., Siebert M., Artymowicz P., 1999, ApJ, 526, 1001.
Lynden-Bell D., Pringle J.E., 1974, MNRAS, 168, 603.
Marcy G.W., Butler R.P., 2000, PASP, 112, 137.
Mathis J.S., Rumpl W., Nordsieck K.H., 1977, apJ, 217, 425.
Matsuyama I., Johnstone D., Hartmann L., 2002, ApJ, in press.
Mayor M., Queloz D., 1995, Nature, 378, 355.
Monaghan J.J., 1992, ARA&A, 30, 543.
Murray J.R., 1996, MNRAS, 279, 402.
Navarro J.F., White S.D.M., 1993, MNRAS, 265, 271.
Nelson A.F., Benz W., Ruzmaikina T.V., 2000, ApJ, 529, 357.
Nelson R.P., Papaloizou J.C.B., Masset F., Kley W., 2000, MNRAS, 318, 18
Pringle J.E., 1981, ARA&A, 19, 137.

Rice W.K.M., Armitage P.J., Bate M.R., Bonnell I.A., 2003, MNRAS, 338, 227.
Schneider G., Wood K., Silverstone M., Hines D.C., Koerner D.W., Whitney B., Bjorkman J.E., Lowrance P.J., 2002, AJ, submitted.
Shakura N.J., Sunyaev R.A., 1973, A&A, 24, 337.
Siess L., Forestini M., Bertout C., 1999, A&A, 342, 480.
Simon M., Prato L., 1995, ApJ, 450, 824.
Simon M., Dutrey A., Guilloteau S., 2000, ApJ, 545, 1034.
Syer D., Clarke C.J., 1996, MNRAS, 278, L23.
Trilling D.E., Benz W., Guillot T., Lunine J.I., Hubbard W.B., Burrows A., 1998, ApJ, 500, 428
Trilling D.E., Lunine J.I., Benz W., 2002, A&A, 394, 241.
Weaver W.B., Jones G., 1992, ApJS, 78, 239.
Wolf S., Gueth F., Henning T., Kley W., 2002, ApJ, 566, L97.
Wood K., Lada C.J., Bjorkman J.E., Kenyon S.J., Whitney B.A., Wolff M.J., 2002a, ApJ, 567, 1138
Wood K., Wolff M.J., Bjorkman J.E., Whitney B.A., 2002b, ApJ, 564, 887

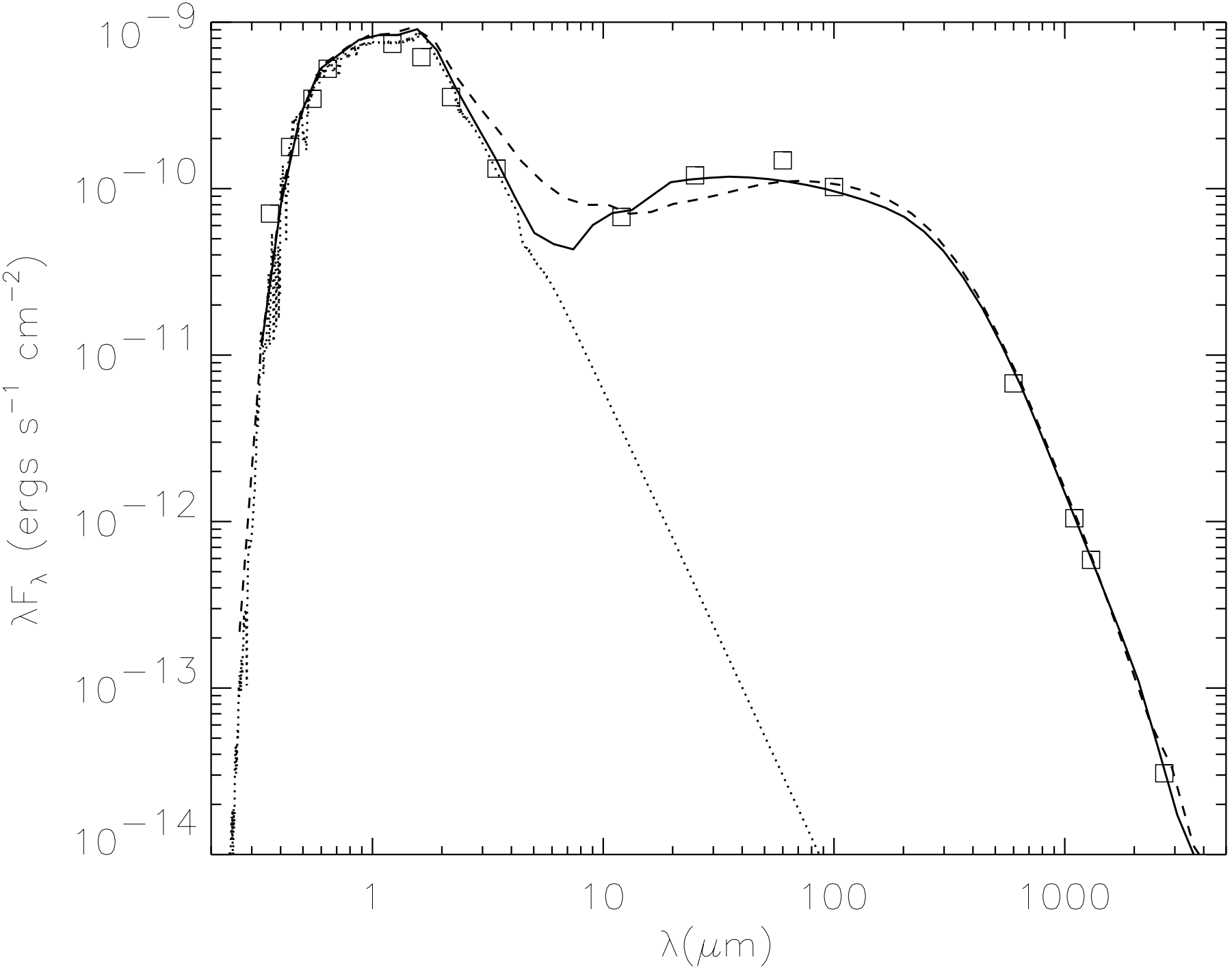
10^{-9}
10^{-10}
10^{-11}
10^{-12}
10^{-13}
10^{-14}
λF_λ (ergs s^{-1} cm^{-2})
1
10
100
1000
$\lambda(\mu m)$

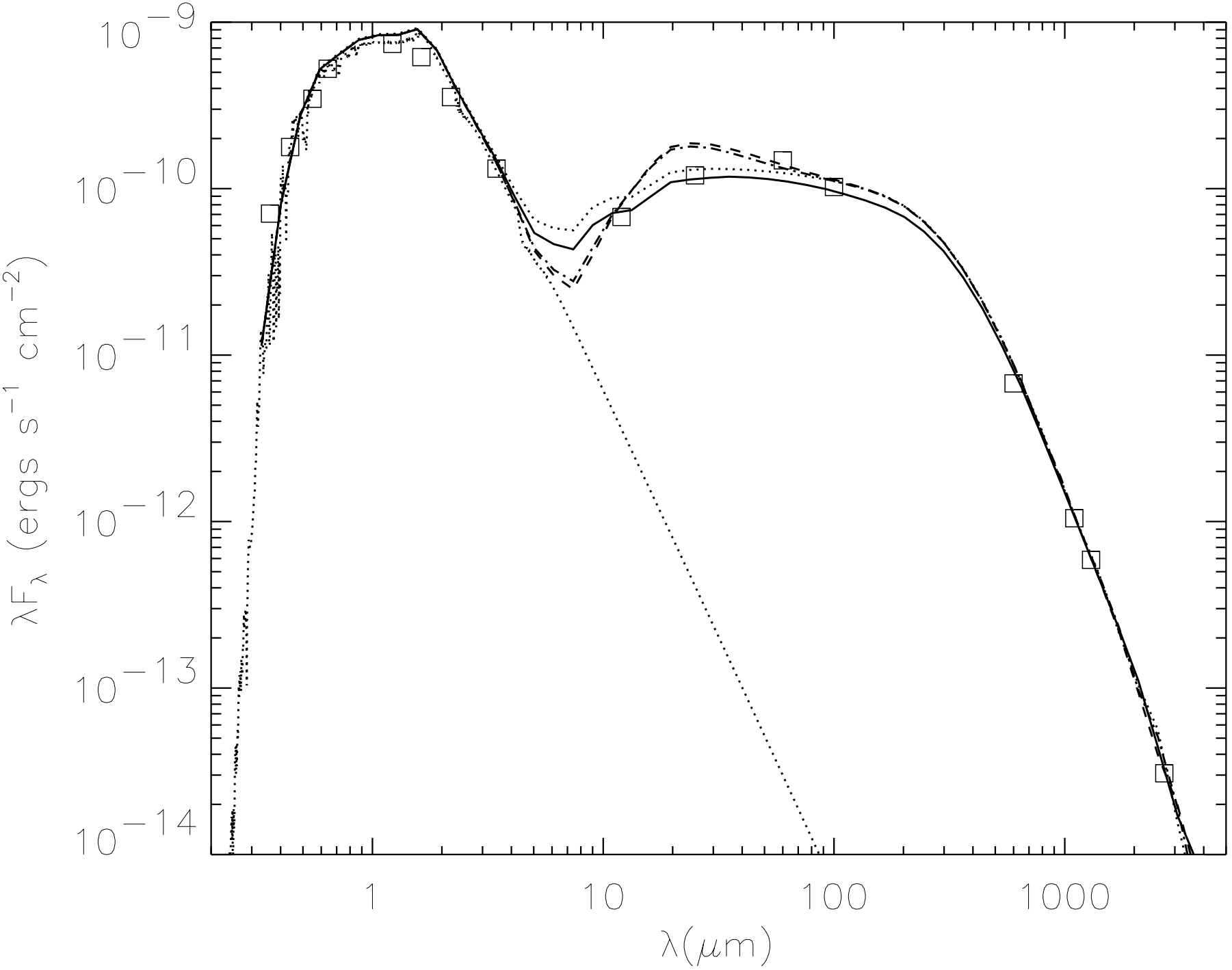
10^{-9}
10^{-10}
10^{-11}
10^{-12}
10^{-13}
10^{-14}
λF_λ (ergs s^{-1} cm^{-2})
1
10
100
1000
$\lambda(\mu m)$

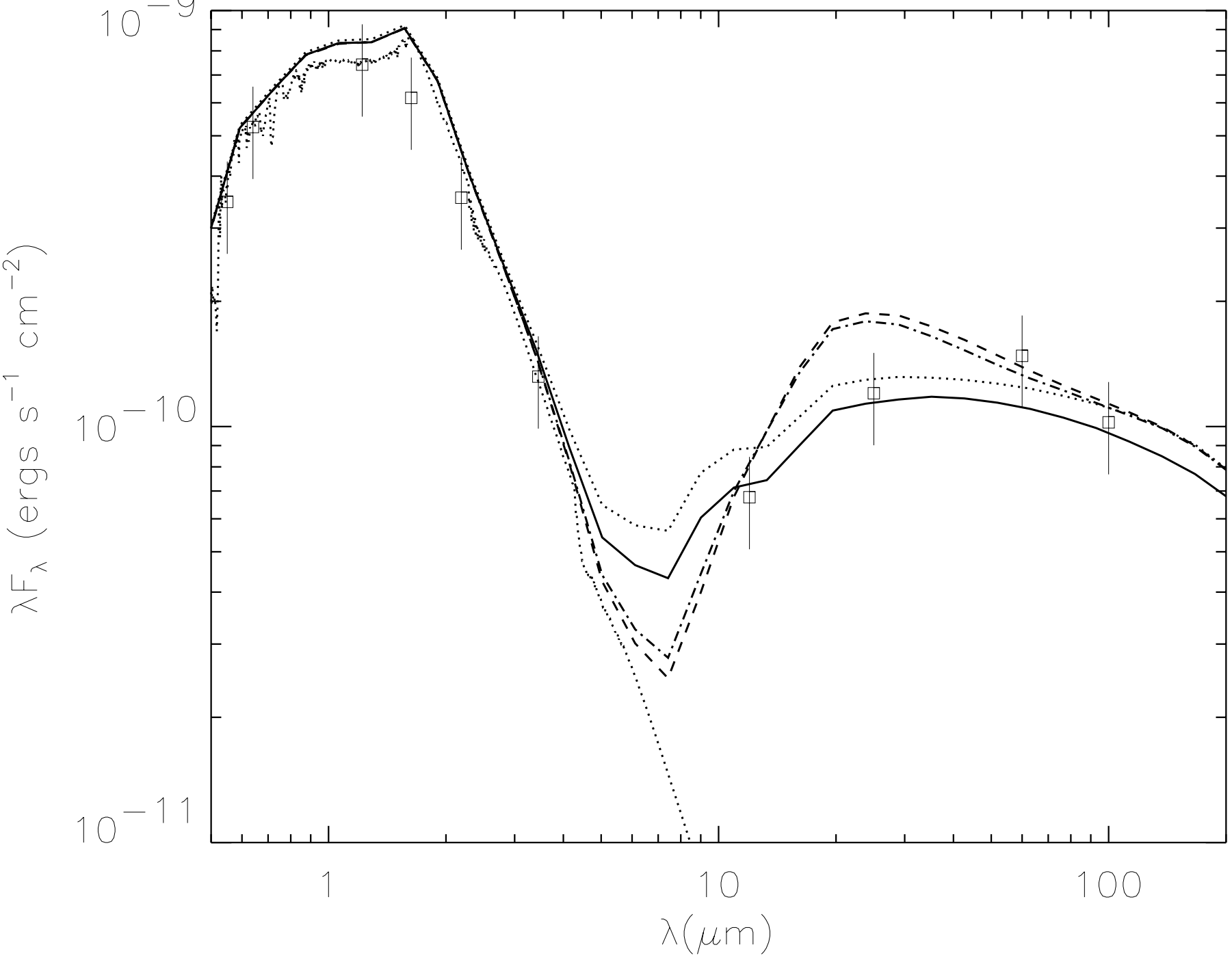
10^{-9}
10^{-10}
10^{-11}
λF_λ (ergs s^{-1} cm^{-2})
1
10
100
$\lambda(\mu m)$